Mon. Not. R. Astron. Soc. **316**, 734–748 (2000)

The magnetosphere of an oscillating neutron star. Non-vacuum treatment

A. N. Timokhin,[1,2,3★†] G. S. Bisnovatyi-Kogan[2] and H. C. Spruit[3]

[1]*Sternberg Astronomical Institute, Universitetskij pr. 13, 119899 Moscow, Russia*
[2]*Space Research Institute, Profsoyuznaya 84/32, 117810 Moscow, Russia*
[3]*Max-Planck-Institut für Astrophysik, Karl-Schwarzschild Str. 1, D-85740 Garching, Germany*

Accepted 2000 March 14. Received 2000 March 6; in original form 1999 September 24

ABSTRACT

We generalize a formula for the Goldreich–Julian charge density ($\rho_{\rm GJ}$), originally derived for a rotating neutron star, for arbitrary oscillations of a neutron star with an arbitrary magnetic field configuration under the assumption of low current density in the inner parts of the magnetosphere. As an application, we consider the toroidal oscillation of a neutron star with a dipole magnetic field and calculate the energy losses. For some oscillation modes, the longitudinal electric field cannot be cancelled by putting charged particles in the magnetosphere without the presence of a strong electric current ($j \simeq \rho_{\rm GJ} c \times c/\omega r$). It is shown that the energy losses are strongly affected by plasma in the magnetosphere, and cannot be described by vacuum formulae.

Key words: stars: magnetic fields – stars: neutron – stars: oscillations – pulsars: general.

1 INTRODUCTION

The oscillations of neutron stars may provide an opportunity to study their internal structure. Oscillations of neutron stars (NS) may be observable in pulsars just after a glitch. The energy release during the glitch is estimated as

$$E \sim \frac{1}{2}\frac{M_{\rm crust}}{M_{\rm NS}} I\Omega^2 \frac{\Delta\Omega}{\Omega}, \qquad (1)$$

where I is the moment of inertia of the NS, Ω is an angular velocity of rotation, $\Delta\Omega$ is a jump of angular velocity, $M_{\rm NS}$ is the mass of the NS and $M_{\rm crust}$ is the mass of the crust. For the Vela pulsar, $E \sim 10^{37}$ erg. There are about 20 glitching pulsars, which have suffered a total of 45 glitches (Lyne 1996). The energy release in each of these glitches is similar to that of the Vela pulsar. If several per cent of this energy went into the excitation of oscillations it would be possible to observe them. Another example of how oscillations of NS could be observed in pulsars is by observations of microstructure in single pulses. Boriakoff (1976) proposed that vibrations of a neutron star may cause the periodicity of micropulses observed in some pulsars. A difficulty in this theory is that no effective mechanism has been proposed for the excitation of oscillations (Hankins 1996).

Oscillating neutron stars have been proposed as a source for Galactic gamma-ray bursts (GRBs) by Pacini & Ruderman (1974) and Tsygan (1975). This idea is further developed by Blaes et al. (1989), Smith & Epstein (1993) and Fatuzzo & Melia (1993). Oscillation-induced hard gamma radiation from NS was proposed by Bisnovatyi-Kogan (1995) and Ding & Cheng (1997) as an explanation of the hard delayed emission observed from some GRBs (Hurley et al. 1994), even if the GRB itself is generated by a different mechanism (Bisnovatyi-Kogan et al. 1975). Recent GRB observations make a Galactic origin for GRBs unlikely, but a Galactic model may not be excluded completely. At least for soft gamma repeaters, which are believed to be neutron stars, oscillations of stars can play an essential role (Duncan 1998).

Eigenfrequencies and eigenfunctions of neutron star oscillations have been computed by many authors (McDermott, Van Horn & Hansen 1988; Carroll et al. 1986; Strohmayer 1991). These calculations have shown that typical periods of neutron star oscillations range from 0.1 up to several tens of ms. On the other hand, observed pulsar radiation in different spectral regions is generated mostly in the magnetosphere (Trümper & Becker 1998). If we are looking for oscillation-induced radiation from pulsars, we should investigate processes in the magnetosphere. A complete solution for vacuum electromagnetic fields near an oscillating magnetized neutron star was obtained by Muslimov & Tsygan (1986). For a typical NS magnetic field strength ($>10^9$ G), however, the electric field arising from the oscillation of a star will be strong enough to pull charged particles from the surface into the magnetosphere. Hence, any realistic model of the magnetosphere of an oscillating NS must take into account the presence of charged particles. This will also affect the electromagnetic energy losses of a pulsating magnetized star. Electromagnetic energy losses of an oscillating NS in vacuum were calculated by McDermott et al. (1984) and Muslimov & Tsygan (1986).

★ Present address: Max-Planck-Institut für Kernphysik, Saupfercheckweg 1, D-69117 Heidelberg, Germany.
† E-mail: andrey.timokhin@mpi-hd.mpg.de

As a first step in the investigation of the magnetosphere of an oscillating neutron star with non-zero charge density, we consider the inner part of the magnetosphere, assuming low current density there. We generalize a formula for the Goldreich–Julian charge density, derived originally for a rotating NS, for a NS oscillating in any arbitrary mode. This allows us to take into account plasma present in the magnetosphere of the NS and calculate the energy losses. The plan of the paper is as follows. In the first section we introduce some definitions and give an algorithm for calculation of the Goldreich–Julian charge density for an arbitrary oscillation mode and magnetic field structure under the assumption of low current density, and discuss the limitations of this assumption. In the second section we apply this formalism to toroidal oscillations of a NS with a dipole magnetic field. We calculate the Goldreich–Julian charge density and energy losses for some oscillation modes and discuss the factors affecting energy losses of an oscillating neutron star.

2 GENERAL FORMALISM

2.1 Basic definitions

As was first pointed out by Goldreich & Julian (1969), a rotating NS cannot be surrounded by a vacuum. The electric field generated by the rotation of magnetized NS will pull charged particles into the magnetosphere – the electrostatic force near the NS surface in a vacuum would be much stronger than the gravitational one for both electrons and ions. According to the calculations of Jones (1986), the binding of charged particles in the crust of a typical pulsar is not strong enough to prevent them being pulled into the magnetosphere by the vacuum electric field. Even if the binding of charged particles in the cold crust of an old NS can prevent the particles escaping, however, the magnetosphere of a strong magnetized neutron star can be filled by charged particles by the mechanism proposed by Ruderman & Sutherland (1975) for pulsars.

On the NS surface, the vacuum electric field generated by rotation or oscillation has a radial component, the value of which is a substantial part of the full field strength (Muslimov & Tsygan 1986; Goldreich & Julian 1969). To an order of magnitude, this field for the rotating star is

$$E^{\rm rot} \simeq \frac{\Omega r_*}{c} B, \tag{2}$$

where Ω is the rotational frequency of the NS, r_* is the NS radius and B is the magnetic field strength near the star. In the case of NS oscillations, the corresponding vacuum electric field is

$$E^{\rm osc} \simeq \frac{\omega \xi}{c} B, \tag{3}$$

where ω is the oscillation frequency and ξ is the displacement amplitude. The vacuum electric field strength near the NS oscillating with period τ will be of the same order as the field strength generated by rotation of the NS with period $T_{\rm eff}$:

$$T_{\rm eff} \simeq \tau \frac{r_*}{\xi}. \tag{4}$$

For typical oscillation parameters (McDermott et al. 1988), the strength of the vacuum electric field of the oscillating NS will be the same as that generated by a $\sim$1 s pulsar. Hence, the magnetosphere of an oscillating, even non-rotating, NS should be filled by charged particles. In the strong magnetic field of the NS ($B > 10^9$ G), synchrotron energy losses of charged particles in the magnetosphere are very high. They lose their perpendicular momentum (if any) very rapidly and occupy the first Landau level, i.e. they can move only along magnetic field lines.

In the presence of strong longitudinal (parallel to $\boldsymbol{B}$) electric field $E_\parallel$, charged particles are accelerated to high energies and their curvature radiation in a strong magnetic field produces an electron–positron pair cascade (Sturrock 1971; Daugherty & Harding 1982). The particles produced in the cascade cancel the accelerating electric field. Because of this, there should be a regular force-free ($E_\parallel \ll B$) configuration of the electromagnetic field, at least in the inner parts of the magnetosphere, where the NS magnetic field is strong enough to allow single photon pair creation:

$$\boldsymbol{E}^{\rm GJ} \cdot \boldsymbol{B} = 0. \tag{5}$$

Let us call the electric field $\boldsymbol{E}^{\rm GJ}$ the Goldreich–Julian (GJ) electric field. We introduce the generalized Goldreich–Julian charge density as the charge density in the magnetosphere corresponding to the GJ electric field $\boldsymbol{E}^{\rm GJ}$:

$$\rho_{\rm GJ} = \frac{1}{4\pi} \nabla \cdot \boldsymbol{E}^{\rm GJ}. \tag{6}$$

It follows from the above discussion that the charge density in the inner parts of the magnetosphere of an oscillating NS should be approximately equal to the GJ charge density.

In the following, we are looking for the GJ electric field and the GJ charge density, because they should adequately describe the electric field and the charge density in the inner parts of the NS magnetosphere. Knowledge of them will allow us to calculate electromagnetic energy losses of an oscillating NS.

2.2 Basic equations: low current density approximation

We assume the neutron star to be a magnetized conducting sphere of radius r_*. We are interested only in the pulsation modes with non-vanishing amplitude ξ on the surface. Consider a region close to the NS (near zone), at distances from the NS surface smaller than the wavelength $\lambda = 2\pi c/\omega$, where ω is the oscillation frequency and c is the speed of light. In the near zone, $r < \lambda$, one can neglect the displacement current term. Maxwell's equations for the electric and magnetic fields in the near zone are

$$\nabla \cdot \boldsymbol{E} = 4\pi\rho, \tag{7}$$

$$\nabla \times \boldsymbol{E} = -\frac{1}{c} \partial_t \boldsymbol{B}, \tag{8}$$

$$\nabla \cdot \boldsymbol{B} = 0, \tag{9}$$

$$\nabla \times \boldsymbol{B} = \frac{4\pi}{c} \boldsymbol{j}, \tag{10}$$

where $\boldsymbol{B}$ and $\boldsymbol{E}$ are the magnetic and electric fields and ρ and $\boldsymbol{j}$ are the charge and current density. We use the notation for partial derivatives $\partial_\alpha \equiv \partial/\partial\alpha$. On the unperturbed surface of the NS, $\boldsymbol{E}$ and $\boldsymbol{B}$ must satisfy the following boundary conditions:

$$B_r(r_*) = B_{0r}, \tag{11}$$

$$B_{\theta,\phi}(r_*) = B_{0\theta,0\phi} \pm \frac{4\pi}{c} \boldsymbol{J}_{\phi,\theta}, \tag{12}$$

$$E_{\theta,\phi}(r_*) = -\frac{1}{c} (\mathbf{V} \times \boldsymbol{B}_0)_{\theta,\phi}, \tag{13}$$

$$E_r(r_*) = -\frac{1}{c} (\mathbf{V} \times \boldsymbol{B}_0)_r + 4\pi\sigma, \tag{14}$$

where the subscripts r, θ, ϕ denote vector components in a spherical coordinate system, $\mathbf{V}$ is the velocity of oscillation of the NS surface, $\boldsymbol{B}_0$ is the surface magnetic field inside the NS, and σ and $\boldsymbol{J}$ are the induced surface charge and current density. Here equations (14) and (12) are used to determinate the surface charge and current densities. Close to the NS, the current flows along the magnetic field lines. Therefore for the inner parts of the magnetosphere it can be expressed as

$$\boldsymbol{j} = \alpha(r, \theta, \phi)\boldsymbol{B}, \tag{15}$$

where α is a scalar function. This system must be completed by equation (5), defining the GJ electric field. We failed to find an analytical solution of the system in the general case. Under some physical assumptions, however, it can be solved analytically for an arbitrary oscillation mode and magnetic field configuration of the NS.

Let us assume that the physical current density in the magnetosphere is low enough that the magnetic field to first order in $\tilde{\xi} \equiv \xi/r_*$ can be considered as generated only by volume currents inside the NS and by surface currents on its surface, i.e.

$$\frac{4\pi}{c}\boldsymbol{j} \ll \nabla \times \boldsymbol{B}^{(1)}, \tag{16}$$

where $\boldsymbol{B}^{(1)}$ is the first order in $\tilde{\xi}$ perturbation of the magnetic field. To an order of magnitude, this means

$$j \ll \frac{1}{r}\left(B^{(0)}\frac{\xi}{r_*}\right)c = \frac{B^{(0)}\omega\xi}{cr_*}c\left(\frac{c}{\omega r}\right), \tag{17}$$

where $B^{(0)}$ is the unperturbed magnetic field strength. The value of the Goldreich–Julian charge density near the surface of the NS is, to an order of magnitude, $\rho_{\rm GJ}(r_*) \simeq B^{(0)}V/(cr_*)$, where V is the oscillation velocity amplitude. Thus equation (16) implies

$$j \ll \rho_{\rm GJ}(r_*)c\left(\frac{c}{\omega r}\right). \tag{18}$$

We call assumption (16) the low current density approximation. For regions of complete charge separation, where there are charged particles of only one sign, the maximum current density is $\rho_{\rm GJ}c$. The absolute value of the Goldreich–Julian charge density decreases with increasing r and in the near zone $r \ll c/\omega$. Consequently condition (18) for a charge-separated solution is satisfied automatically. Charged particles in the near zone move along magnetic field lines. Therefore the current flowing through a field line tube remains the same. Because of this, condition (18) is automatically satisfied along field lines that have crossed a region of charge separation. For regions in the near zone, where there are charged particles of different sign and the magnetic field lines have not crossed a charge-separated region, condition (18) *can* be violated.

We assume that condition (18) is satisfied in the whole near zone and find the GJ electric field and the GJ charge density. For some oscillation modes, the $\rho_{\rm GJ}$ obtained under this assumption has singularities. For the reasons discussed in Section 2.2, a regular solution of the system (5), (7)–(15) should exist for any oscillation mode and unperturbed magnetic field configuration of a NS. Hence, in cases where *our* solution has singularities, the low current density approximation fails and the physical current cannot be neglected in the whole near zone. In some regions the current density will be, to an order of magnitude,

$$j \simeq \rho_{\rm GJ}(r_*)c\left(\frac{c}{\omega r}\right). \tag{19}$$

This situation will be considered in subsequent papers. As we will show, the small current density approximation holds in regions of open field lines. In the whole near zone it is valid for more than 50 per cent of the modes, at least for toroidal oscillations of a NS with a dipole magnetic field.

2.3 Goldreich–Julian charge density

2.3.1 Equations for the Goldreich–Julian charge density

In the low current density approximation, one can neglect the current term in Ampere's law (10). To the first order of the dimensionless oscillation amplitude $\tilde{\xi}$ in the near zone, we have

$$\nabla \times \boldsymbol{B} = 0. \tag{20}$$

Using the properties of solenoidal vector fields, we write $\boldsymbol{B}$ in the form

$$\boldsymbol{B} = \nabla \times \nabla \times (P\boldsymbol{e}_r) + \nabla \times (Q\boldsymbol{e}_r), \tag{21}$$

where $\boldsymbol{e}_r = \boldsymbol{r}/r$. Scalar functions P and Q can be expanded in spherical harmonics Y_{lm} as

$$P(\boldsymbol{r}, t) = \sum_{lm}\tilde{P}_{lm}(r, t), Y_{lm}(\theta, \phi) \tag{22}$$

$$Q(\boldsymbol{r}, t) = \sum_{lm}\tilde{Q}_{lm}(r, t)Y_{lm}(\theta, \phi). \tag{23}$$

Substituting $\boldsymbol{B}$ in the form (21) into equation (20) and multiplying the result by $\boldsymbol{e}_r$, we obtain

$$\Delta_\Omega Q = 0, \tag{24}$$

where Δ_Ω is the angular part of the Laplacian,

$$\Delta_\Omega \equiv \frac{1}{\sin\theta}\partial_\theta(\sin\theta\partial_\theta) + \frac{1}{\sin^2\theta}\partial_{\phi\phi}. \tag{25}$$

Substitution of the expansion (23) into equation (24) gives us $\tilde{Q}_{lm} \equiv 0$ for each l,m. Hence, $Q \equiv 0$ (see Muslimov & Tsygan 1986) and the magnetic field can be expressed in terms of only one scalar function P as

$$\boldsymbol{B} = \nabla \times \nabla \times (P\boldsymbol{e}_r). \tag{26}$$

Substituting for $\boldsymbol{B}$ using expression (26) in Faraday's law (8), we obtain

$$\nabla \times \boldsymbol{E} = -\frac{1}{c}\nabla \times \nabla \times (\partial_t P\boldsymbol{e}_r). \tag{27}$$

Integrating this equation, we find

$$\boldsymbol{E} = -\frac{1}{c}\nabla \times (\partial_t P\boldsymbol{e}_r) - \nabla\Psi, \tag{28}$$

where Ψ is an arbitrary scalar function.

From the theory of partial differential equations (Elsgolts 1965; Brandt 1947) it is known that for any vector field $\boldsymbol{A}$ there exists a vector field perpendicular to $\boldsymbol{A}$ if and only if

$$\boldsymbol{A} \cdot (\nabla \times \boldsymbol{A}) = 0. \tag{29}$$

From equation (20), it follows that magnetic $\boldsymbol{B}$ satisfies equation (29) and there always exists a vector field perpendicular to $\boldsymbol{B}$. Let us assume that there exists an *electric* field $\boldsymbol{E}^{\rm GJ}$ with no component parallel to $\boldsymbol{B}$, satisfying the boundary conditions (13), (14). Evidently it satisfies Maxwell's equations (7)–(20), and consequently has the form

$$\boldsymbol{E}^{\rm GJ} = -\frac{1}{c}\nabla \times (\partial_t P\boldsymbol{e}_r) - \nabla\Psi_{\rm GJ}. \tag{30}$$

The electric field $\boldsymbol{E}^{\rm GJ}$ satisfies equation (5). Substituting for $\boldsymbol{E}^{\rm GJ}$ using expression (30) in the equality (5), we have an equation for $\Psi_{\rm GJ}$:

$$\frac{1}{c}\nabla\times(\partial_t P\boldsymbol{e}_r)\cdot\boldsymbol{B}+\nabla\Psi_{\rm GJ}\cdot\boldsymbol{B}=0. \tag{31}$$

Substituting for $\boldsymbol{E}^{\rm GJ}$ from the expression (30) in equality (6), we obtain an expression for the GJ charge density in terms of the GJ potential $\Psi_{\rm GJ}$:

$$\rho_{\rm GJ}=-\frac{1}{4\pi}\Delta\Psi_{\rm GJ}. \tag{32}$$

In other words, if one uses representation (26) for a magnetic field in the near zone, then the Goldreich–Julian electric field is written as a sum of two terms (30). The first one is the vacuum term, and the second one $(-\nabla\Psi_{\rm GJ})$ represents the contribution of the charged particles in the magnetosphere of the NS. The potential $\Psi_{\rm GJ}$ is a solution of equation (31). In spherical coordinates, equation (31) becomes (using expression 26)

$$\Delta_\Omega P\partial_r\Psi_{\rm GJ}-\partial_r\partial_\theta P\partial_\theta\Psi_{\rm GJ}-\frac{1}{\sin^2\theta}\partial_r\partial_\phi P\partial_\phi\Psi_{\rm GJ}$$
$$+\frac{1}{c\sin\theta}(\partial_r\partial_\phi P\partial_\theta\partial_t P-\partial_r\partial_\theta P\partial_\phi\partial_t P)=0. \tag{33}$$

Let us consider small oscillations of a NS, $\tilde{\xi}\ll 1$. We expand the function P in a series in $\tilde{\xi}$ and approximate it by the sum of the first two terms:

$$P(t,r,\theta,\phi)\approx P_0(r,\theta,\phi)+\delta P(t,r,\theta,\phi), \tag{34}$$

where the function $P_0(r,\theta,\phi)$ is responsible for the unperturbed magnetic field and $\delta P(t,r,\theta,\phi)$ is the first-order term in an expansion of $P(t,r,\theta,\phi)$ in $\tilde{\xi}$. We expand δP in series of spherical harmonics

$$\delta P=\sum_{l,m}\delta\tilde{p}_{lm}(t,r)Y_{lm}(\theta,\phi). \tag{35}$$

Subsequently we will need only the time derivative of δP. After substitution of the expansion (35) in equation (20) we find (see Appendix A)

$$\partial_t\delta P=\sum_{l,m}\left(\frac{r_*}{r}\right)^l\partial_t\delta p_{lm}(t)Y_{lm}(\theta,\phi). \tag{36}$$

The coefficients $\partial_t\delta p_{lm}(t)$ are fixed by the boundary conditions.

2.3.2 *Boundary conditions*

The boundary conditions for the potential $\Psi_{\rm GJ}$ are obtained from the boundary conditions for electric field (13). The tangential components of the GJ electric field on the surface of the NS are

$$E^{\rm GJ}_\theta|_{r=r_*}=\frac{1}{c}\frac{1}{r}\left(\frac{1}{r}\Delta_\Omega P v_\phi+\frac{1}{\sin\theta}\partial_r\partial_\phi P v_r\right)\Big|_{r=r_*}, \tag{37}$$

$$E^{\rm GJ}_\phi|_{r=r_*}=-\frac{1}{c}\frac{1}{r}\left(\frac{1}{r}\Delta_\Omega P v_\theta+\partial_r\partial_\theta P v_r\right)\Big|_{r=r_*}. \tag{38}$$

From expression (30), the tangential components of the GJ electric field outside the NS are

$$E^{\rm GJ}_\theta=-\frac{1}{r}\left(\frac{1}{c}\frac{1}{\sin\theta}\partial_\phi\partial_t P+\partial_\theta\Psi_{\rm GJ}\right), \tag{39}$$

$$E^{\rm GJ}_\phi=\frac{1}{r}\left(\frac{1}{c}\partial_\theta\partial_t P-\frac{1}{\sin\theta}\partial_\phi\Psi_{\rm GJ}\right). \tag{40}$$

Equating these expressions on the surface of the NS and expressing $\Psi_{\rm GJ}$, one obtains boundary conditions for the θ and ϕ derivatives of $\Psi_{\rm GJ}$:

$$\partial_\theta\Psi_{\rm GJ}|_{r=r_*}=-\frac{1}{c}$$
$$\times\left(\frac{1}{r}\Delta_\Omega P v_\phi+\frac{1}{\sin\theta}\partial_r\partial_\phi P v_r+\frac{1}{\sin\theta}\partial_\phi\partial_t P\right)\Big|_{r=r_*}, \tag{41}$$

$$\partial_\phi\Psi_{\rm GJ}|_{r=r_*}=\frac{1}{c}\sin\theta$$
$$\times\left(\frac{1}{r}\Delta_\Omega P v_\theta+\partial_r\partial_\theta P v_r+\partial_\theta\partial_t P\right)\Big|_{r=r_*}. \tag{42}$$

From these boundary conditions we obtain the boundary condition to be applied to $\delta p_{lm}(t)$. Differentiating equation (41) with respect to ϕ and equation (42) with respect to θ and equating results, we obtain an expression for $\delta p_{lm}(t)$ to first order in $\tilde{\xi}$ (see Appendix B),

$$\partial_t\delta p_{lm}(t)=\frac{1}{l(l+1)}\int_{4\pi}{\rm d}\Omega Y^*_{lm}[\mathbf{V}\cdot\nabla(\Delta_\Omega P_0)+\Delta_\Omega P_0(\nabla\cdot\mathbf{V}_\perp)$$
$$+r^2(\nabla_\perp(\partial_r P_0)\cdot\nabla_\perp)v_r]|_{r=r_*}. \tag{43}$$

The boundary condition for $\Psi_{\rm GJ}$ can be obtained by integrating equation (41) or equation (42). For convenience we will use as boundary condition the result of integrating equation (41) over θ. For a perturbation depending on time t as $\mathrm{e}^{-\mathrm{i}\omega t}$ we obtain, to first order in $\tilde{\xi}$,

$$\Psi_{\rm GJ}|_{r=r_*}=-\frac{1}{c}\int{\rm d}\theta$$
$$\times\left(\frac{1}{r}\Delta_\Omega P_0 v_\phi+\frac{1}{\sin\theta}\partial_r\partial_\phi P_0 v_r+\frac{1}{\sin\theta}\partial_\phi\partial_t\delta P\right)\Big|_{r=r_*}$$
$$+\mathrm{e}^{-\mathrm{i}\omega t}F(\phi), \tag{44}$$

where F is a function of ϕ.

For each oscillation mode, the corresponding velocity field is continuously differentiable. From the boundary condition for the electric field (13), it follows that the tangential components of $\boldsymbol{E}^{\rm GJ}$ are finite. The vacuum term on the right-hand side in expression (30) for the electric field $\boldsymbol{E}^{\rm GJ}$ is also finite [with the natural assumption that P is continuously differentiable with respect to θ and ϕ expressions (43) and (36) are finite for $r=r_*$]. Let us consider the azimuthal component of GJ electric field $E^{\rm GJ}_\phi$ near the poles.[1] In expression (40) for $E^{\rm GJ}_\phi$ outside the NS, both $E^{\rm GJ}_\phi$ and the first (vacuum) term on the right-hand side of expression (40) are finite. Consequently the second term

$$-\frac{\partial_\phi\Psi_{\rm GJ}}{\sin\theta}\Big|_{r=r_*}$$

is also finite, hence $\partial_\phi\Psi_{\rm GJ}|_{\{\theta=0,\pi;r=r_*\}}=0$. Thus in the boundary condition (44) one must choose F such that $\Psi_{\rm GJ}|_{\theta=0,\pi;r=r_*}=C_{1,2}\mathrm{e}^{-\mathrm{i}\omega t}$, where $C_{1,2}$ are some constants. Using the gauge freedom, we choose

$$\Psi_{\rm GJ}|_{\theta=0;r=r_*}=0. \tag{45}$$

[1] Points with $\theta=0(\pi), r=r_*$.

Using approximation (34) for P, we write an equation for $\Psi_{\rm GJ}$ in the case of small oscillations:

$$\Delta_\Omega P_0 \partial_r \Psi_{\rm GJ} - \partial_r \partial_\theta P_0 \partial_\theta \Psi_{\rm GJ} - \frac{1}{\sin^2\theta}\partial_r \partial_\phi P_0 \partial_\phi \Psi_{\rm GJ} + \frac{1}{c\sin\theta}(\partial_r \partial_\phi P_0 \partial_\theta \partial_t \delta P - \partial_r \partial_\theta P_0 \partial_\phi \partial_t \delta P) = 0. \quad (46)$$

The first-order partial differential equation (46), together with the boundary conditions (44), (45) and $\partial_t \delta P$ described by formulae (36) and (43), determines $\Psi_{\rm GJ}$. The solution of this problem provides $\Psi_{\rm GJ}$ to first order in $\tilde{\xi}$. The Goldreich–Julian charge density $\rho_{\rm GJ}$ can then be obtained from the formula (32).

2.4 Rotating NS – pulsar

Finally, in this section we consider an important particular case – a rotating neutron star. We choose the z axis to be parallel to the rotation axis. In this case the partial derivative ∂_t can be replaced by $-\Omega\partial_\phi$, where Ω is the angular velocity. Thus

$$\partial_t P = -\Omega \partial_\phi P. \quad (47)$$

Equation (33) for $\Psi_{\rm GJ}$ takes the form

$$\Delta_\Omega P \partial_r \Psi_{\rm GJ} - \partial_r \partial_\theta P \partial_\theta \Psi_{\rm GJ} - \frac{1}{\sin^2\theta}\partial_r \partial_\phi P \partial_\phi \Psi_{\rm GJ} - \frac{\Omega}{c}\frac{1}{\sin\theta}(\partial_r \partial_\phi P \partial_\theta \partial_\phi P - \partial_r \partial_\theta P \partial_{\phi\phi} P) = 0. \quad (48)$$

By direct substitution of

$$\Psi_{\rm GJ}^{\rm rot} = -\frac{\Omega}{c}\sin\theta \partial_\theta P, \quad (49)$$

it can be shown that the potential (49) is a solution of equation (48), and satisfies the boundary conditions (41, 42). We note that equation (33) and its particular form (48), and boundary conditions (41, 42), are valid for an arbitrary oscillation amplitude, i.e. also for rotation of the NS. Substituting potential $\Psi_{\rm GJ}^{\rm rot}$ into the expression for the GJ electric field (30), one obtains

$$\boldsymbol{E}_{\rm GJ}^{\rm rot} = -\frac{1}{c}(\boldsymbol{\Omega}\times\boldsymbol{r})\times\boldsymbol{B}. \quad (50)$$

This result was obtained by Goldreich & Julian (1969) and Mestel (1971).

3 DIPOLE MAGNETIC FIELD – TOROIDAL OSCILLATIONS

3.1 General formulae

As an application of the developed formalism, we consider the case of small-amplitude toroidal oscillations of a NS with dipole magnetic field. The velocity field on the NS surface for a toroidal oscillation mode (l, m) is described by (Unno et al. 1979)

$$v_r = 0,$$
$$v_\theta = \mathrm{e}^{-\mathrm{i}\omega t} W(r)\frac{1}{\sin\theta}\partial_\phi Y_{lm}(\theta,\phi),$$
$$v_\phi = -\mathrm{e}^{-\mathrm{i}\omega t} W(r)\partial_\theta Y_{lm}(\theta,\phi), \quad (51)$$

where W is the transverse velocity amplitude. For simplicity we assume that the mode axis is aligned with the dipole moment $\boldsymbol{\mu}$. We can do this without loss of generality, because any oscillation mode with the mode axis not aligned with the dipole moment can be represented by a series of oscillation modes with the mode axis parallel to $\boldsymbol{\mu}$. In this case the unperturbed magnetic field is

$$\boldsymbol{B} = B_0\left(\frac{r_*}{r}\right)^3 \cos\theta \boldsymbol{e}_r + \frac{1}{2}B_0\left(\frac{r_*}{r}\right)^3 \sin\theta \boldsymbol{e}_\theta, \quad (52)$$

where $\boldsymbol{e}_r$ and $\boldsymbol{e}_\theta$ are unit coordinate vectors. This field is described by the scalar function $P_0^{\rm dip}$ (see equations 26 and 34) according to the formulae (A7) and (A8):

$$P_0^{\rm dip} = \frac{B_0 r_*^3}{2r}\cos\theta. \quad (53)$$

The scalar function $\delta P^{\rm dip}$ (see equation 34) describes the first order in $\tilde{\xi}$ magnetic field perturbation. The time derivative of this function for an oscillation mode (l, m), according to formulae (36), (B7), is

$$\partial_t \delta P_{lm}^{\rm dip} = B_0 w r_* \frac{1}{l(l+1)}\left(\frac{r_*}{r}\right)^l \partial_\phi Y_{lm}, \quad (54)$$

where $w \equiv \mathrm{e}^{-\mathrm{i}\omega t} W$. Substituting $P_0^{\rm dip}$ and $\partial_t \delta P_{lm}^{\rm dip}$ into the general equation (46), we obtain a partial differential equation for the GJ potential $\Psi_{\rm GJ}^{lm}$ for a NS with a dipole magnetic field oscillating with a small amplitude in a toroidal mode (l, m):

$$2\cos\theta\partial_r \Psi_{\rm GJ}^{lm} + \frac{1}{r}\sin\theta\partial_\theta \Psi_{\rm GJ}^{lm} - \frac{m^2}{l(l+1)}\frac{B_0 w}{c}\left(\frac{r_*}{r}\right)^{l+1} Y_{lm} = 0, \quad (55)$$

where $\Psi_{\rm GJ}^{lm}$ corresponds to one excited oscillation mode (l, m), and for the general mode $\Psi_{\rm GJ} = \sum_{lm}\Psi_{\rm GJ}^{lm}$. The characteristics of the equation (55) are

$$t = C_0,$$
$$\phi = C_1,$$
$$\sin\theta\left(\frac{r_*}{r}\right)^{1/2} = C_2,$$
$$\Psi_{\rm GJ}^{lm} - \frac{m^2}{l(l+1)}\frac{B_0 w r_*}{c}\left(\frac{r_*}{r}\right)^l \sin^{2l}\theta \int \frac{Y_{lm}}{(\sin\theta)^{2l+1}}\mathrm{d}\theta = C_3. \quad (56)$$

The integral of equation (55) is an arbitrary function of constants C_0, C_1, C_2, C_3,

$$\varphi(C_0, C_1, C_2, C_3) = 0. \quad (57)$$

Expressing $\Psi_{\rm GJ}^{lm}$, we have for the general solution of equation (55)

$$\Psi_{\rm GJ}^{lm} = \frac{m^2}{l(l+1)}\frac{B_0 w r_*}{c}\left(\frac{r_*}{r}\right)^l \sin^{2l}\theta \times \int \frac{Y_{lm}}{(\sin\theta)^{2l+1}}\mathrm{d}\theta + \Phi_{lm}\left[\sin\theta\left(\frac{r_*}{r}\right)^{1/2}, \phi, t\right], \quad (58)$$

where Φ is an arbitrary function. In order for $\Psi_{\rm GJ}^{lm}$ represented by the expression (58) to be a GJ potential, it must satisfy the boundary conditions on the surface of the NS (44) and (45), which in the case of toroidal oscillations of a NS with dipole magnetic field take the form

$$\Psi_{\rm GJ}^{lm}|_{r=r_*} = -\frac{B_0 w r_*}{c}\int\left[\cos\theta\partial_\theta Y_{lm} - \frac{m^2}{l(l+1)}\frac{Y_{lm}}{\sin\theta}\right]\mathrm{d}\theta + \mathrm{e}^{-\mathrm{i}\omega t}F(\phi), \quad (59)$$

$$\Psi_{\rm GJ}^{lm}|_{\theta=0, r=r_*} = 0. \quad (60)$$

Substituting the $\Psi_{\rm GJ}^{lm}$ given by expression (58) into the boundary conditions (59), (60), we obtain the boundary condition for the function Φ^{lm}:

$$\Phi^{lm}\left(\sin\theta\left(\frac{r_*}{r}\right)^{1/2},\phi,t\right)\Big|_{r=r_*} =$$
$$-\frac{B_0 w r_*}{c}\int\left(\cos\theta\,\partial_\theta Y_{lm}-\frac{m^2}{l(l+1)}\frac{Y_{lm}}{\sin\theta}\right)\mathrm{d}\theta$$
$$-\frac{B_0 w r_*}{c}\frac{m^2}{l(l+1)}\sin^{2l}\theta\int\frac{Y_{lm}}{(\sin\theta)^{2l+1}}\mathrm{d}\theta$$
$$+\frac{B_0 w r_*}{c}\left[\int\left(\cos\theta\,\partial_\theta Y_{lm}-\frac{m^2}{l(l+1)}\frac{Y_{lm}}{\sin\theta}\right)\mathrm{d}\theta\right]\Big|_{\theta=0}, \qquad (61)$$

where the last term is added in order to satisfy the second boundary condition (60). The function Φ^{lm} depends on θ in the combination $(r_*/r)^{1/2}\sin\theta$. To obtain Φ^{lm}, one has to express the right-hand side of equation (61) in terms of $\sin\theta$, and to replace $\sin\theta$ by $(r_*/r)^{1/2}\sin\theta$. Substituting the function Φ^{lm} into the expression (58), we obtain the potential $\Psi_{\rm GJ}^{lm}$ for small toroidal oscillations of a NS with a dipole magnetic field for the mode (l,m). Using the formula (32), we obtain the Goldreich–Julian charge density for that mode. We have developed a set of programs using the computer algebra language MATHEMATICA 3.0 (Wolfram 1996) for calculating the analytical expressions of $\rho_{\rm GJ}^{lm}$ according to the algorithm described in this section. These programs were tested for some (l,m) by comparing results obtained by hand and by computer, and also by checking the condition $\boldsymbol{E}^{\rm GJ}\cdot\boldsymbol{B}=0$.

3.2 Main results

3.2.1 Goldreich–Julian charge density

In the solution for the whole region, the expression (61) is used, where on the right-hand side $\cos\theta$ should be replaced by $[1-(\frac{r_*}{r})\sin^2\theta]^{1/2}$ for $0\leqslant\theta<\pi/2$ (first hemisphere) and by $-[1-(\frac{r_*}{r})\sin^2\theta]^{1/2}$ for $\pi/2\leqslant\theta\leqslant\pi$ (second hemisphere). Because of this, there are two different expressions for $\Psi_{\rm GJ}$ for both hemispheres. If these expressions give different results for $\theta=\pi/2$ for $r>r_*$, there is a discontinuity in the function $\Psi_{\rm GJ}$ at the equatorial plane, and consequently $\rho_{\rm GJ}(r,\pi/2,\phi)$ becomes infinite. As we discussed in Section 2.2, this unphysical result indicates that the low current density approximation for such oscillation modes cannot be applied in the whole near zone. In this situation it is impossible to cancel the accelerating electric field in the whole near zone without the presence of a strong electric current (19) in

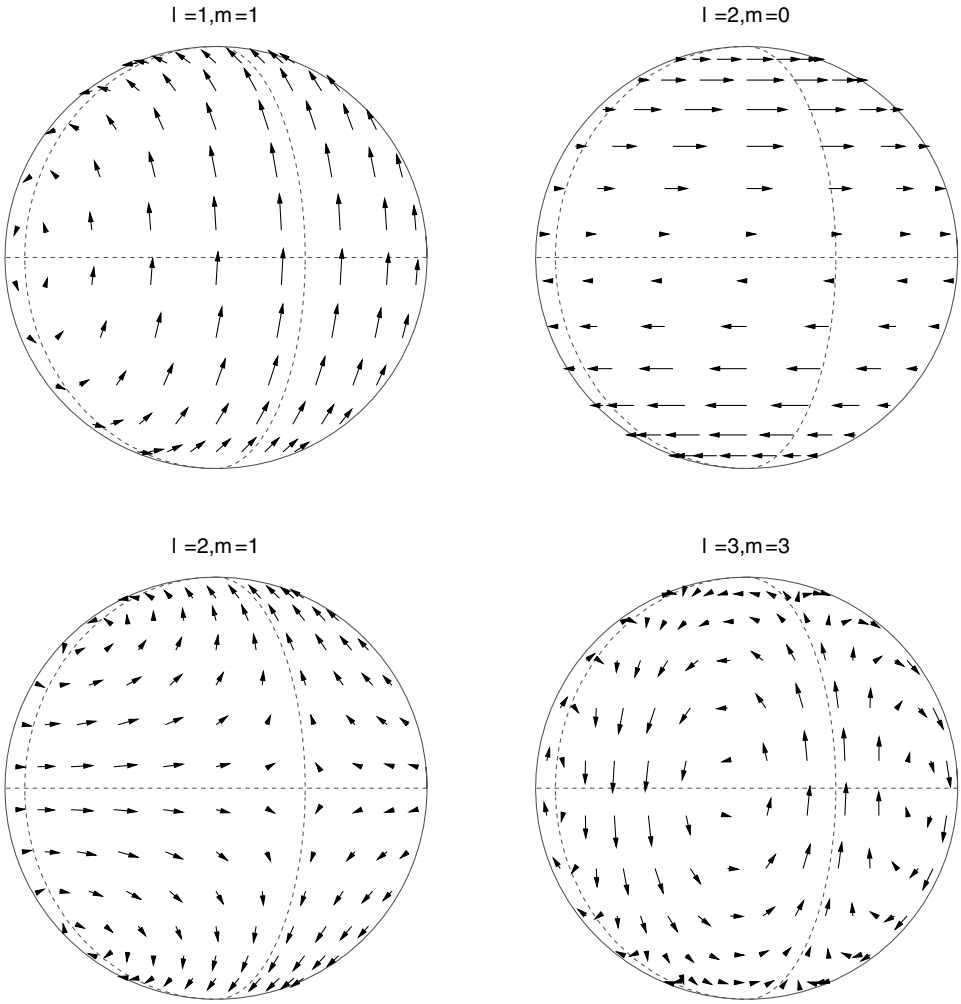

Figure 1. Velocity field on a sphere for toroidal modes (1, 1), (2, 0), (2, 1) and (3, 3), shown at time $t=2\pi n/\omega$, where n is an integer, as a projection on the meridional plane $\phi=-115°$. Circles corresponding to the longitudes 0° (right), −90° (left) and latitude 0° are shown by dashed lines.

some magnetospheric regions. Examples of such oscillation modes are modes $(l, m) = (2, 0)$, $(3, 3)$. The corresponding velocity fields are given in Fig. 1. The dependence of the potential $\Psi_{\rm GJ}^{lm}$ for these modes along dipole magnetic field lines is shown in Figs 2 and 3. In the following we normalize the GJ potential $\Psi_{\rm GJ}$ and charge density $\rho_{\rm GJ}$ by $B_0 W r_*/c$ and $B_0 W/r_* c$, respectively. The size of the discontinuity in $\Psi_{\rm GJ}(r, \pi/2, \phi)$ decreases as the angle at which the corresponding magnetic field line intersect the surface of the NS increases. $\Psi_{\rm GJ}$ is a continuous function of θ on the surface of the NS; nevertheless, the GJ charge density diverges on the equator even on the surface of NS (see Figs 4 and 5). In these figures, the charge density $\rho_{\rm GJ}^{lm}|_{r=r_*}$ is shown in spherical coordinates $(|\rho_{\rm GJ}^{lm}|_{r=r_*}|, \theta, \phi)$. Here the radial coordinate represents the absolute value of the GJ charge density as a function of the polar angle θ and the azimuthal angle ϕ. Analytical expressions for the GJ charge density for the discussed modes are given in Appendix C. At the equatorial plane

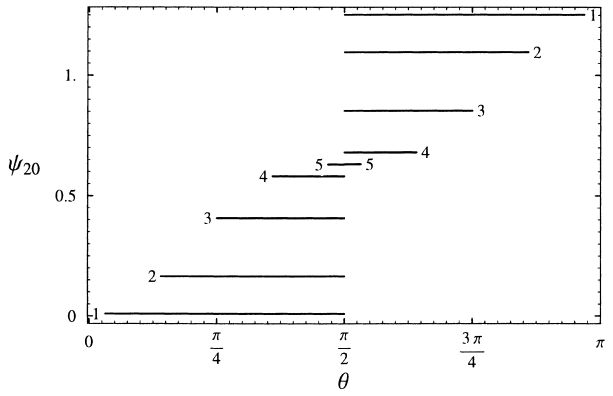

Figure 2. The potential $\Psi_{\rm GJ}^{20}$ along a dipolar magnetic field line as a function of the polar angle θ is shown for 5 field lines for $t = 2\pi n/\omega$, at which the maximal absolute values of the potential are reached. The values of θ for the left and right ends of the lines 1–5 determine the polar angle at which the corresponding magnetic field line crosses the surface of the neutron star. The discontinuity is shown by the jump of ψ corresponding to the same field line in the opposite hemisphere.

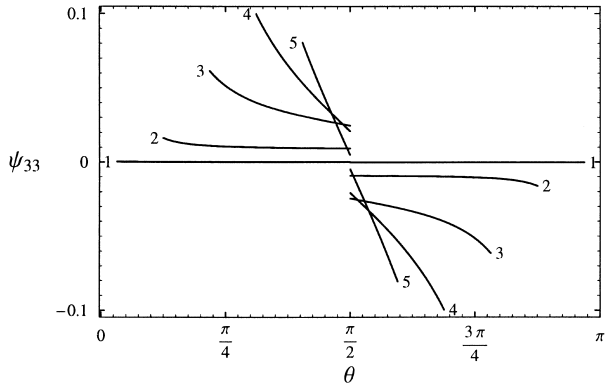

Figure 3. The potential $\Psi_{\rm GJ}^{33}$ along a dipolar magnetic field line as a function of the polar angle θ is shown for 5 field lines with azimuthal angle $\phi = \pi/6$, for $t = 2\pi n/\omega$, at which the maximal absolute values of the potential are reached. The values of θ for the left and right ends of the lines 1–5 determine the polar angle at which the corresponding magnetic field line crosses the surface of the neutron star. The discontinuity is shown by the jump of ψ corresponding to the same field line in the opposite hemisphere.

$\rho_{\rm GJ}^{lm}$ is infinite. The mode $(2, 1)$ is a representative of another class of oscillation modes, in which $\Psi_{\rm GJ}^{lm}$ is a continuous function of θ (see Fig. 6) and $\rho_{\rm GJ}^{lm}$ is finite everywhere. The velocity field and $\rho_{\rm GJ}^{21}$ are shown in Figs 1 and 7. For such modes, it is possible to cancel the longitudinal electric field without generating a strong current along the magnetic field lines.

Consider now the difference between two classes of toroidal oscillation modes for a NS with a dipole magnetic field. The boundary condition for $\Psi_{\rm GJ}^{lm}$ is proportional to the vector product of $\mathbf{V}$ and $\boldsymbol{B}$. The axis z is directed along the dipole magnetic momentum. If the velocity field is symmetric relative to the equatorial plane ($l - m$ is an odd number), then the boundary condition for $\Psi_{\rm GJ}^{lm}$ is also symmetric relative to the equatorial plane. Hence, after expression of all trigonometric functions in equation (61) in terms of $\cos\theta$ and $\sin\theta$, $\cos\theta$ appears on the right-hand side of equation (61) only in even powers. Consequently, the function Φ^{lm} will be the same in both hemispheres and $\rho_{\rm GJ}^{lm}$ will be finite. If velocity field is antisymmetric relative to the equatorial plane ($l - m$ is an even number or zero), then $\cos\theta$ is contained in the right-hand side of equation (61) in odd powers, the function Φ^{lm} may have a discontinuity in the plane $\theta = \pi/2$, and $\rho_{\rm GJ}^{lm}$ for such modes becomes infinite at the equatorial plane. An example of an oscillation mode with a velocity field that is antisymmetric relative to the equatorial plane and for which $\Psi_{\rm GJ}^{lm}$ is a continuous function of θ is the mode $(1, 1)$. Diagrams for the potential $\Psi_{\rm GJ}^{11}$ and Goldreich–Julian charge density $\rho_{\rm GJ}^{11}$ are shown in Figs 8 and 9. Therefore for a dipole magnetic field the longitudinal electric field generated by the oscillation modes with odd $(l - m)$ can be cancelled by placing charged particles in the magnetosphere. Among the modes with even or zero $(l - m)$, there are modes for which the longitudinal electric field cannot be cancelled by the placement of charged particles without the presence of a strong electric current along some magnetic field lines.

For an oscillation mode with odd $(l - m)$ there is a regular solution for $\rho_{\rm GJ}$ and $\boldsymbol{E}^{\rm GJ}$ in the low current density approximation. This solution will be stable because of Lenz's law: increasing the current will lead to generation of a magnetic field, inducing an electric field, which will prevent the current from growing. In other words, the configuration with the smallest possible current will exist. For oscillation modes with even or zero $(l - m)$, where no regular solution for the GJ charge density and electric field exists, the low current density approximation cannot be used in the whole near zone. Because some of the oscillation modes in this class (at least one) possess a regular solution in the low current density approximation, the total percentage of modes for which this approximation may be used in the whole near zone exceeds 50 per cent.

The Goldreich–Julian charge density gives only a characteristic charge density in the magnetosphere. The particle density can be obtained by solving the full system of MHD equations, but this has not been done even for an aligned rotator with a dipole magnetic field (Michel 1991). The case of non-radial oscillation is much more complicated, because of the absence of stationarity and axial symmetry. Regarding the particle number density in the region of closed magnetic field lines, we can say that for oscillation modes with odd $(l - m)$ there can be charge-separated regions in the near zone. For such modes, the potential on the foot points of magnetic field lines has the same sign and there are regions where GJ charge density does not change the sign along the whole magnetic field line. Hence, charged particles of only one sign can be pulled from the NS surface into these

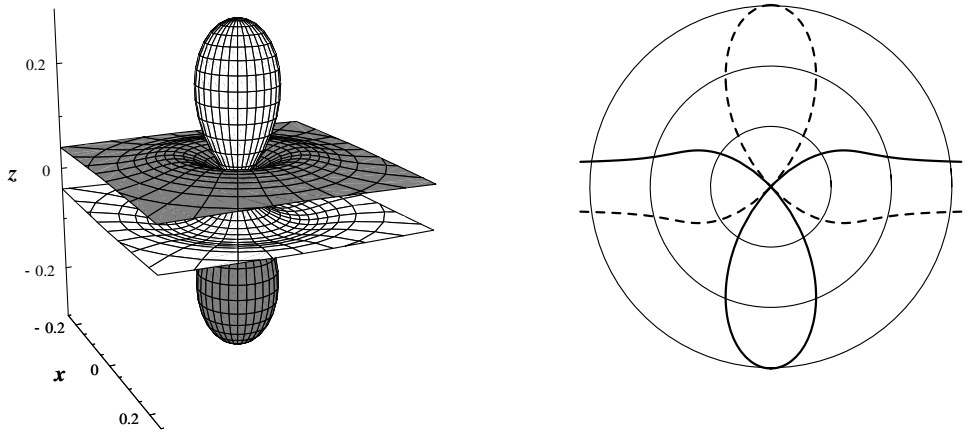

Figure 4. Left: the charge density $\rho^{20}_{\rm GJ}|_{r=r_*}$ is shown in a spherical coordinate system $(|\rho^{lm}_{\rm GJ}|_{r=r_*}|, \theta, \phi)$ for $t = 2\pi n/\omega$. The radial coordinate represents the absolute value of the GJ charge density as a function of the polar angle θ and the azimuthal angle ϕ. Positive values of the charge density are shown by a grey surface and negative ones by white. The dipole magnetic moment $\boldsymbol{\mu}$ is directed upwards along the z axis. The azimuthal angle is counted from the x axis, as in Fig. 1. Note that for $\theta = \pi/2$, $\rho^{20}_{\rm GJ}$ is infinite. Right: the section of surfaces from the left figure by a meridional plane. Circles correspond to the values 0.1, 0.2 and 0.3. Positive values are shown as solid lines, negative ones as dashed. Note that for $\theta = \pi/2$, $\rho^{20}_{\rm GJ}$ is infinite.

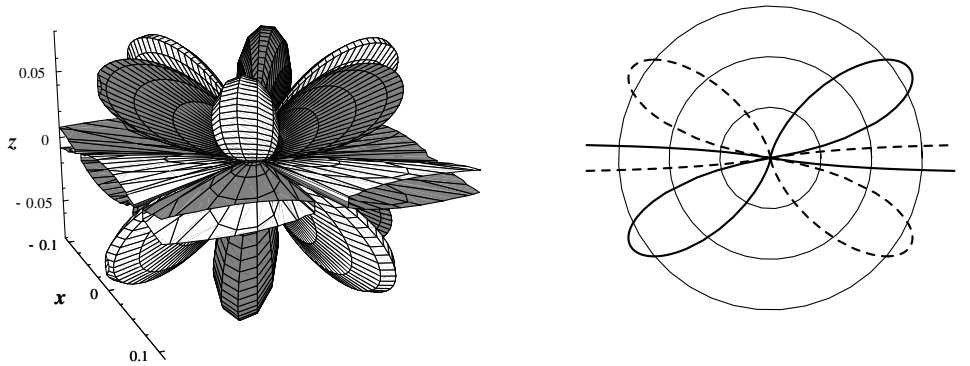

Figure 5. Left: the charge density $\rho^{33}_{\rm GJ}|_{r=r_*}$ is shown in a spherical coordinate system $(|\rho^{lm}_{\rm GJ}|_{r=r_*}|, \theta, \phi)$ for $t = 2\pi\, n/\omega$. The radial coordinate represents the absolute value of the GJ charge density as a function of the polar angle θ and the azimuthal angle ϕ. Positive values of charge density are shown by a grey surface and negative ones by a white one. The dipole magnetic moment $\boldsymbol{\mu}$ is directed upwards along the z axis. The azimuthal angle is measured from the x axis, as in Fig. 1. Note that for $\theta = \pi/2$, $\rho^{33}_{\rm GJ}$ is infinite. Right: the section of surfaces from the left figure by the plane $\phi = \pi/6$, where the maximal absolute values of the charge density $\rho^{33}_{\rm GJ}|_{r=r_*}$ are reached. Circles correspond to the values 0.04, 0.08 and 0.12. Positive values are shown solid, negative ones dashed. Note that for $\theta = \pi/2$, $\rho^{33}_{\rm GJ}$ is infinite.

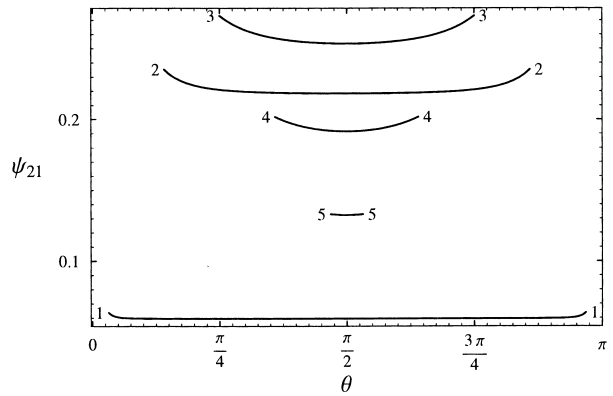

Figure 6. The potential $\Psi^{21}_{\rm GJ}$ along a dipolar magnetic field line as a function of the polar angle θ is shown for 5 field lines with azimuthal angle $\phi = \pi/2$, for $t = 2\pi n/\omega$, at which the maximal absolute values of the potential are reached. The values of θ for the left and right ends of the lines 1–5 determine the polar angle at which the corresponding magnetic field line crosses the surface of the neutron star.

regions. Evidently for modes with even or zero $(l - m)$ there cannot be charge-separated regions in the near zone, because the GJ charge density changes the sign along any magnetic field line.

3.2.2 Energy losses

In previous works, the calculation of electromagnetic energy losses of an oscillating neutron star includes only radiation of electromagnetic waves in the vacuum. If there is plasma in the magnetosphere, then the energy will be lost by transformation of the oscillation energy into kinetic energy of an outflowing plasma, as was proposed for pulsar energy losses by Goldreich & Julian (1969). They obtained the energy losses of a rotating aligned NS through outflow of the charged particles from a region of open field lines, and found it to be equal to the loss in vacuum through radiation of electromagnetic waves by a perpendicular rotator. In this paper we consider electric and magnetic fields in the near zone; hence we cannot explicitly show the existence of a plasma outflow as in the aligned rotator of Goldreich & Julian, but

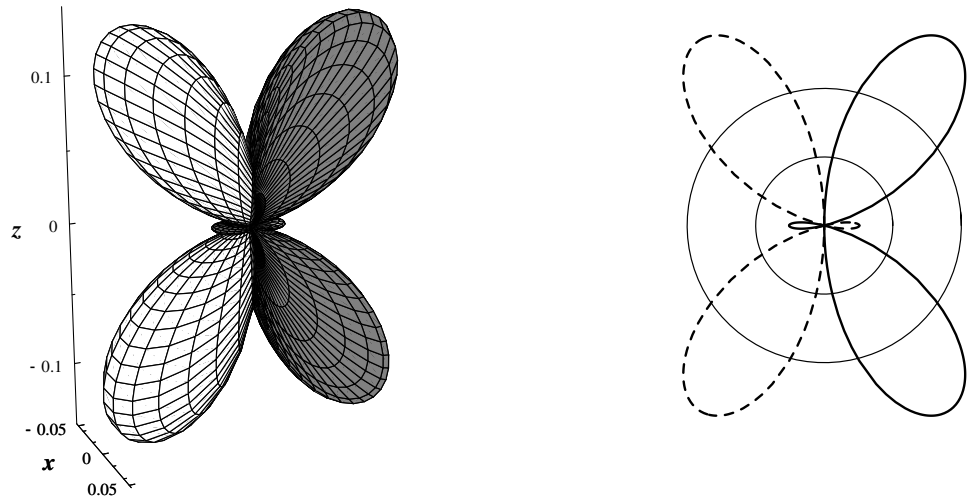

Figure 7. Left: the charge density $\rho^{21}_{\rm GJ}|_{r=r_*}$ is shown in a spherical coordinate system ($|\rho^{lm}_{\rm GJ}|_{r=r_*}|, \theta, \phi$) for $t = 2\pi n/\omega$. The radial coordinate represents the absolute value of the GJ charge density as a function of the polar angle θ and the azimuthal angle ϕ. Positive values of charge density are shown by a grey surface and negative ones by a white one. The dipole magnetic moment $\boldsymbol{\mu}$ is directed upwards along the z axis. The azimuthal angle is measured from the x axis, as in Fig. 1. Right: the section of surfaces from the left figure by the plane $\phi = \pi/2$, where the maximal absolute values of the charge density $\rho^{21}_{\rm GJ}|_{r=r_*}$ are reached. Circles correspond to the values 0.05, 0.1 and 0.15. Positive values are shown as solid lines, negative ones as dashed lines.

qualitatively the picture is as follows. The electric current arising from the motion of the charged particles in the magnetosphere generates a magnetic field. On the Alfvenic surface, in the region where the value of this field becomes larger than the unperturbed NS magnetic field, the field lines become open. Plasma escaping from the region of open field lines produces an electromagnetically driven stellar wind. The wind causes a net electric current, which closes at infinity. This current flows beneath the stellar surface between positive and negative emission regions. Because it must cross magnetic field lines there, it exerts a braking torque on the oscillating NS and reduces the oscillational energy. This picture is similar to the one proposed by Ruderman & Sutherland (1975) for pulsars, but now we must obtain the boundary of the open field line region self-consistently. In our case we cannot approximate the closed field line region by a 'zone of corotation'; rather we should self-consistently determine the last closed field line as the last field line lying inside the Alfven surface.

Consider the region near the pole. Let us use θ_0 to denote the polar angle by which the last closed field line intersects the surface of the NS. Similarly to the case of pulsars above a polar cap, an acceleration zone and a zone of e^+–e^- pair generation above it will be built. Electron–positron pairs cancel the accelerating electric field, i.e. the motion of a charged particle above the accelerating zone will be not influenced by the electric field generated by stellar oscillations. In the region of open field lines, where particles escape from the neutron star and form a relativistic wind, the average time of crossing of the acceleration zone by a particle is much less then the oscillation period (see Discussion), so particles in practice do not return to the star. Hence, averaged over the oscillation period, the energy loss through the outflow of plasma from the open field line region is

$$\epsilon^{lm}_{\rm pl} \simeq \frac{1}{\tau}\int_0^\tau {\rm d}t \int_0^{2\pi}\int_0^{\theta_0} |j^{lm}(r_*, \theta, \phi) A^{lm}(\theta, \phi)| r_*^2 \sin\theta \, {\rm d}\theta \, {\rm d}\phi, \qquad (62)$$

where $A(\theta, \phi)$ is the work done by the electric field to move a unit charge to the point with coordinate $(r*, \theta, \phi)$:

$$A(\theta, \phi) \simeq \int_0^\theta E^{\rm GJ}_\theta(r_*, \theta', \phi) r_* \, {\rm d}\theta'. \qquad (63)$$

For reasons discussed at the end of Section 2.2, the charge density in the inner parts of the magnetosphere must be approximately equal to the Goldreich–Julian charge density $\rho_{\rm GJ}$. In the region of plasma outflow, charged particles are streaming along magnetic field lines in the same direction with ultrarelativistic velocities. The charge density of the outflowing plasma is equal to the Goldreich–Julian charge density. Hence, an outflowing ultrarelativistic electron–positron plasma builds a net current density

$$j \simeq \rho_{\rm GJ} c. \qquad (64)$$

The current density can differ from the values given by expression (64), because of differences in the averaged velocities of electron and positron components of the plasma (for discussion on this topic see Lyubarskii 1992), but the order-of-magnitude expression (64) gives a good estimate for the current density (Ruderman & Sutherland 1975). Hence, for the open field line region condition (18) is satisfied and in expression (64) we can use the $\rho_{\rm GJ}$ obtained by solving equation (46) for any oscillation mode.

The last closed field line is the line for which the kinetic energy density of the outflowing plasma at the equator [at the point $(R_{\rm a}, \pi/2, \phi)$] becomes equal to the corresponding energy density of the NS magnetic field:

$$\frac{\epsilon^{lm}_{\rm pl}(\theta_0)}{4\pi R_{\rm a}^2 c} \simeq \left.\frac{B^2}{8\pi}\right|_{\theta=\frac{\pi}{2}, r=R_{\rm a}}. \qquad (65)$$

Expressing the right-hand side of this equation in terms of angle θ_0, we obtain two equations (62), (65) for a self-consistent determination of θ_0 and $\epsilon^{lm}_{\rm pl}$.

We have solved these equations for oscillation modes (1,1), (2, 0) and (3, 0). Oscillation periods[2] were taken from McDermott et al. (1988). The ratio of energy losses to the vacuum ones as a function of the amplitude of the dimensionless transverse displacement $\tilde{\xi}$ for modes (1,1), (2,0) and (3,0) is given in Table 1. One can see that energy losses through an outflowing plasma are

[2] According to McDermott et al. (1988), the dependence of the eigenfrequency on l is very weak, at least for small l, so we assumed the same oscillation periods for modes (2, 0) and (3, 0).

much less than those in a vacuum for small values of $\tilde{\xi}$. On the other hand, for oscillation modes $l \geqslant 2$, for displacement amplitudes $\tilde{\xi}$ larger than a value $\tilde{\xi}_{\rm cr}$, energy losses exceed the vacuum losses (see Fig. 10). For some oscillation modes for which $\theta_0 \ll 1$, we can linearize equations (62) and (65) in θ_0 and obtain an analytical estimation of θ_0. For toroidal oscillation mode (l, m), the velocity amplitude V near the pole is of the order

$$V \sim W \begin{cases} \theta^{m-1}, & m \neq 0, \\ \theta, & m = 0. \end{cases} \tag{66}$$

The electric field is of the order $E^{\rm GJ} \sim BV/c$. From formula (63) we have

$$A \sim \frac{BWr_*}{c} \begin{cases} \theta^m, & m \neq 0, \\ \theta^2, & m = 0. \end{cases} \tag{67}$$

The Goldreich–Julian charge density is

$$\rho_{\rm GJ} \sim \frac{BW}{r_* c} \cdot \theta^m \tag{68}$$

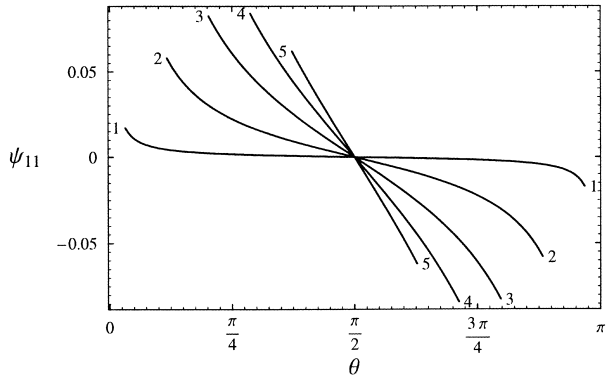

Figure 8. The potential $\Psi^{11}_{\rm GJ}$ along a dipolar magnetic field line as a function of the polar angle θ is shown for 5 field lines with azimuthal angle $\phi = \pi/2$, for $t = 2\pi n/\omega$, at which the maximal absolute values of the potential are reached. The values of θ for the left and right ends of the lines 1–5 determine the polar angle at which the corresponding magnetic field line crosses the surface of the neutron star.

Substituting expressions (67) and (68) into equations (64), (63) and (62), we obtain the energy loss through the plasma outflow along open field lines:

$$\epsilon_{\rm pl} \sim B_0^2 r_*^2 c \left(\frac{W}{c}\right)^2 \begin{cases} \theta_0^{2m+2}, & m \neq 0, \\ \theta_0^4, & m = 0. \end{cases} \tag{69}$$

The angle θ_0 is determined from equation (65). After substitution of $\epsilon_{\rm pl}$ into equation (65), we obtain

$$\theta_0 \sim \begin{cases} \left(\frac{W}{c}\right)^{\frac{1}{3-m}}, & m \neq 0, \\ \left(\frac{W}{c}\right)^{\frac{1}{2}}, & m = 0. \end{cases} \tag{70}$$

We see that the angle θ_0 is small only for modes with $m < 3$. This is because of the small value of V in the polar region for modes with $m \geqslant 3$. For such modes a linear analysis is not possible and the case of large θ_0 needs additional investigation, which will be given elsewhere. The energy loss resulting from plasma outflow is

$$\epsilon_{\rm pl} \sim B_0^2 r_*^2 c \begin{cases} \tilde{\xi}^{\frac{8}{3-m}} \left(\frac{r_* \omega}{c}\right)^{\frac{8}{3-m}}, & m = 1, 2, \\ \tilde{\xi}^4 \left(\frac{r_* \omega}{c}\right)^4, & m = 0. \end{cases} \tag{71}$$

Table 1. Leading terms in the expansion over $\tilde{\xi}$ of the ratio of electromagnetic energy loss through plasma outflow to that in a vacuum $\epsilon_{\rm pl}/\epsilon_{\rm vac}$, and the distance in the equatorial plane of the last closed field line to the wavelength $R^{lm}_{\rm a}/\lambda$ for toroidal oscillation modes $(1, 1)$, $(2, 0)$ and $(3, 0)$. τ is the period of oscillations in ms.

Mode	$\epsilon_{\rm pl}/\epsilon_{\rm vac}$	$R^{lm}_{\rm a}/\lambda$
$(1, 1)$	$0.02\tilde{\xi}^2$	$0.9/\tilde{\xi}$
$(2, 0)$	$77\tilde{\xi}^2\tau^2$	$0.2/\tilde{\xi}$
$(3, 0)$	$9 \times 10^5 \tilde{\xi}^2 \tau^4$	$0.09/\tilde{\xi}$

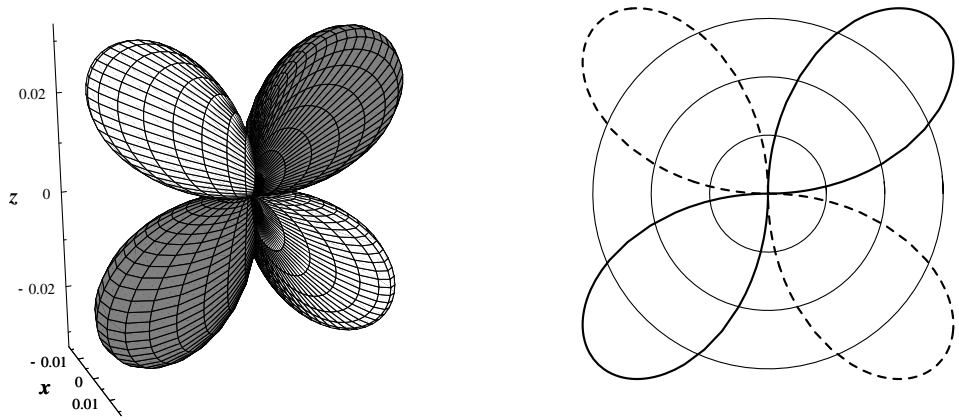

Figure 9. Left: the charge density $\rho^{11}_{\rm GJ}|_{r=r_*}$ is shown in a spherical coordinate system $(|\rho^{lm}_{\rm GJ}|_{r=r_*}|, \theta, \phi)$ for $t = 2\pi n/\omega$. The radial coordinate represents the absolute value of the GJ charge density as a function of the polar angle θ and the azimuthal angle ϕ. Positive values of charge density are shown by a grey surface and negative ones by a white one. The dipole magnetic moment $\boldsymbol{\mu}$ is directed upwards along the z axis. The azimuthal angle is measured from the x axis, as in Fig. 1. Right: the section of surfaces from the left figure by the plane $\phi = \pi/2$, where the maximal absolute values of the charge density $\rho^{11}_{\rm GJ}|_{r=r_*}$ are reached. Circles correspond to the values 0.01, 0.02 and 0.03. Positive values are shown as solid lines, negative ones as dashed lines.

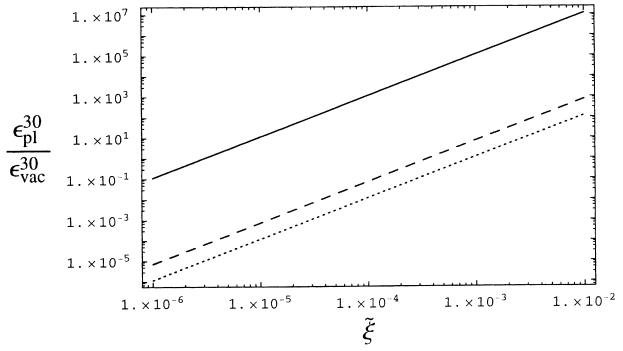

Figure 10. The ratio of the energy loss through outflow of plasma from the region of open field lines to the loss in vacuum is shown as a function of the dimensionless displacement amplitude $\tilde{\xi}$ for the mode (3,0). The solid line corresponds to the oscillation period $T = 19$ ms (mode ${}_3t_0$ in the notation of McDermott et al. 1988), the dashed line to $T = 1.7$ ms (mode ${}_3t_1$) and the dotted line to $T = 1.08$ ms (mode ${}_3t_2$); see note in Section 3.2.2.

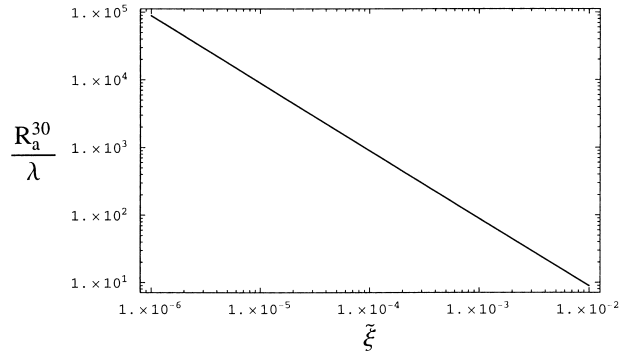

Figure 11. The ratio of the equatorial radius of the last closed field line to the wavelength λ is shown as a function of the dimensionless displacement amplitude $\tilde{\xi}$ for the mode $(3, 0)$. This ratio does not depend on the oscillation frequency ω.

The vacuum energy loss for the oscillation mode (l, m), according to McDermott et al. (1984), is

$$\epsilon_{\rm vac} \sim B_0^2 r_*^2 c \tilde{\xi}^2 \begin{cases} \left(\frac{r_*\omega}{c}\right)^8, & l = 1, m = 0, \\ \left(\frac{r_*\omega}{c}\right)^{2l+2}, & l = 1, m = 1; l \geqslant 2, m = 0 \ldots l. \end{cases} \tag{72}$$

From these formulae we obtain the oscillation amplitude $\tilde{\xi}$ for which the plasma energy loss is larger than the vacuum loss:

$$\tilde{\xi} > \tilde{\xi}_{\rm cr} \sim \begin{cases} \left(\frac{r_*\omega}{c}\right)^2, & l = 1, m = 0, \\ \left(\frac{r_*\omega}{c}\right)^{l-1}, & l \geqslant 2, m = 0; l \geqslant 1, m = 1, \\ \left(\frac{r_*\omega}{c}\right)^{l/3-1}, & l \geqslant 2, m = 2. \end{cases} \tag{73}$$

From formula (73) it follows that for modes $(l = 1, m = 0)$, $(l \geqslant 2,\ m = 0, 1)$ and $(l \geqslant 4, m = 2)$, non-vacuum energy loss exceeds the vacuum loss even for small displacement amplitudes $\tilde{\xi}$, because for these modes $\tilde{\xi}_{\rm cr} \ll 1$.

Electromagnetic waves radiated by the oscillating NS are screened by the plasma. For small $\tilde{\xi}$ the non-vacuum energy loss according to equation (73) is smaller than the vacuum loss, because at the GJ density of particles the accelerated plasma cannot escape from the magnetosphere. The ratio of the equatorial radius for the last closed field line to the wavelength λ is given in Table 1. For mode (3,0), this dependence is shown in Fig. 11. We see that the last closed field line for small values of the displacement amplitude lies deep inside the wave zone. In the region limited by the last closed field lines and a sphere of radius λ (formal boundary of the wave zone) in this situation, confined plasma waves such as Alfven or magnetosonic waves are excited by the oscillation of the NS; see Fig. 12. This will lead to accumulation of energy in this region in the form of plasma wave energy. When the density of this energy becomes larger than that of the magnetic energy, the field lines become open. These

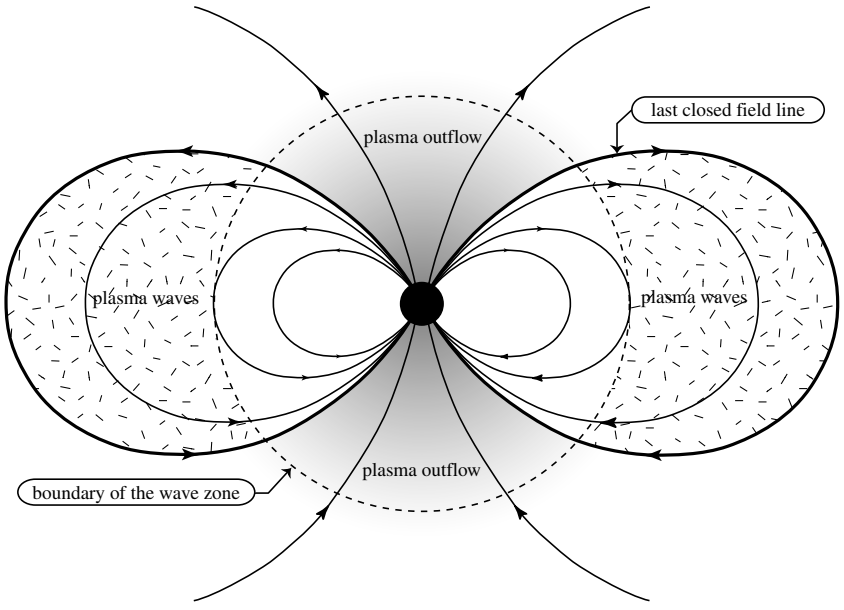

Figure 12. Structure of the magnetosphere of an oscillating neutron star (arbitrary scale). See explanations in the text.

processes will lead to a decrease of the equatorial radius of the last closed field lines, and hence an increase in the energy loss.

A second process that could lead to larger energy losses than obtained by the solution of equation (65) is rotation of the neutron star. In this case the equatorial radius of the last closed field line is the radius of the light cylinder $R_L = \Omega/c$, and the surface area for plasma outflow may be considerably increased. It is not clear, however, how the interaction between rotation and oscillation will influence the total energy losses.

4 DISCUSSION

Under the assumption of low current density, we have developed a formalism describing the inner parts of the magnetosphere of an oscillating neutron star in the same way as in the case of rotation. This assumption is valid in the region of open field lines for any oscillation mode. For some oscillation modes the assumption about low current density everywhere in the inner magnetosphere leads to unphysical results – the Goldreich–Julian charge density becomes infinite at some points. For such oscillation modes, the low current density approximation cannot be used in the whole region of closed magnetic field lines near the NS. The current density for these modes along some closed magnetic field lines will be of the order of magnitude $j \simeq \rho_{\rm GJ} c \times c/(\omega r)$. For a rotating neutron star, our formalism yields the same values for the Goldreich–Julian charge density and electric field as obtained in the works of Goldreich & Julian (1969) and Mestel (1971).

We applied the general formalism to the case of toroidal oscillations of a neutron star with a dipole magnetic field. We calculated the GJ charge density and showed that for the case considered, the assumption about low current density in the whole inner magnetosphere is valid for more than half of all modes. We calculated the electromagnetic energy losses of a NS with a dipole magnetic field for some toroidal oscillation modes and showed that the energy losses of an oscillating neutron star are strongly affected by the plasma present in its magnetosphere. The electromagnetic energy losses of an oscillating NS resulting from plasma outflow from the magnetosphere have in general a different dependence on the oscillation frequency ω and the dimensionless displacement amplitude $\tilde{\xi}$ from the energy losses resulting from radiation of electromagnetic waves in a vacuum. This affects all previous calculations of the electromagnetic damping rate of NS oscillations. Our calculations give a lower limit on the electromagnetic energy losses of an oscillating NS, for the reasons discussed at the end of Section 3.2.2. The energy of oscillation of a star depends on the dimensionless displacement amplitude as $\tilde{\xi}^2$. Energy losses through plasma outflow, in contrast to energy losses through the radiation of electromagnetic waves in a vacuum, have a different dependence on the displacement amplitude. Consequently the electromagnetic energy losses of an oscillating NS in general depend on the oscillation amplitude $\tilde{\xi}$. To estimate the oscillation damping time for the considered oscillation modes, one can use the values given in table 6 of McDermott et al. (1988), multiplying by functions from Table 1 of this paper for a given displacement amplitude. Here we have restricted ourselves to the simple case of toroidal oscillations. Starquakes should excite a whole spectrum of oscillations, including p and g modes. The magnetosphere structure produced by these modes will be considered in a future paper.

With the proposed formalism, it is possible to apply theoretical models developed for pulsars to oscillating neutron stars. For example, one can investigate the acceleration mechanism proposed by Scharlemann, Arons & Fawley (1978) or Ruderman & Sutherland (1975) for oscillating neutron star. The inertial frame dragging mechanism proposed by Muslimov & Tsygan (1992) does not work here, because we consider a non-rotating star. The characteristic time of pair cascade formation is estimated as $h_{\rm PPF}/c$, where $h_{\rm PPF}$ is the height of the pair formation front above the surface. In the 'Ruderman–Sutherland' model, the minimum value of $h_{\rm PPF}$ is the same as for a NS rotating with the angular frequency $\Omega_{\rm eff} = \omega\xi$, and for the usual assumed parameters of a NS, the oscillation is of the order of 10^4–10^5 cm. In an 'Arons–Scharlemann' like model, the height of the pair formation front can be smaller than in a pulsar rotating with the angular frequency $\Omega_{\rm eff}$ (several km), because in general for non-radial oscillations, ratio $\rho_{\rm GJ}/B$ along magnetic field lines increases faster than in the magnetosphere of a rotating NS, which leads to larger accelerating electric fields. Because the characteristic time of pair cascade formation is much shorter than the period of oscillation, one can consider the polar cap acceleration zone at any given moment of time as stationary. The problem of the return current region for the case of an oscillating NS, as in the case of a pulsar, remains open. Similarly to the case of pulsars, the return current can flow along the last closed magnetic field line.

ACKNOWLEDGMENTS

The authors thank A. I. Tsygan for helpful discussions. This work has been supported by the Russian Foundation of Basic Research (RFFI) under grants 96-02-16553 and 99-02-18180.

REFERENCES

Bisnovatyi-Kogan G. S., 1995, ApJS, 97, 185
Bisnovatyi-Kogan G. S., Imshennik V. S., Nadiozhin D. K., Chechetkin V. M., 1975, Ap&SS, 35, 23
Blaes O., Blandford R., Goldreich P., Madau P., 1989, ApJ, 343, 839
Boriakoff V., 1976, ApJ, 208, L43
Brandt L., 1947, Vector and Tensor Analysis. John Wiley & Sons Inc., New York
Carroll B. W., Zweibel E. G., Hansen C. J., McDermott P. N., Savedoff M. P., Thomas J. N., Van Horn H. M., 1986, ApJ, 305, 767
Daugherty J. K., Harding A. K., 1982, ApJ, 252, 337
Ding K. Y., Cheng K. S., 1997, MNRAS, 287, 671
Duncan R. C., 1998, ApJ, 498, L45
Elsgolts L. E., 1965, Differentsialnye uravneniya i variatsionnoe ischislenie. Nauka, Moskva (in Russian)
Fatuzzo M., Melia F., 1993, ApJ, 407, 680
Goldreich P., Julian W. H., 1969, ApJ, 157, 869
Hankins T. H., 1996, in Johnston S., Walker M. A., Bailes M., eds, ASP Conf. Ser. Vol. 105, IAU Colloq. 160, Pulsars: Problems and Progress. Astron. Soc. Pac., San Francisco, p. 197
Hurley K. et al., 1994, Nat, 372, 652
Jones P. B., 1986, MNRAS, 218, 477
Lyne A. G., 1996, in Johnston S., Walker M. A., Bailes M., eds, ASP Conf. Ser. Vol. 105, IAU Colloq. 160, Pulsars: Problems and Progress. Astron. Soc. Pac., San Francisco, p. 73
Lyubarskii Yu. E., 1992, A&A, 261, 544
McDermott P. N., Savedoff M. P., Van Horn H. M., Zweibel E. G., Hansen C. J., 1984, ApJ, 281, 746
McDermott P. N., Van Horn H. M., Hansen C. J., 1988, ApJ, 325, 725
Mestel L., 1971, Nat. Phys. Sci., 233, 149
Michel F. C., 1991, Theory of neutron star magnetospheres. Univ. Chicago Press, Chicago
Muslimov A. G., Tsygan A. I., 1986, Ap&SS, 120, 27
Muslimov A. G., Tsygan A. I., 1992, MNRAS, 255, 61

Pacini F., Ruderman M., 1974, Nat, 251, 399
Ruderman M. A., Sutherland P. G., 1975, ApJ, 196, 51
Scharlemann E. T., Arons J., Fawley W. M., 1978, ApJ, 222, 297
Smith I. A., Epstein R. I., 1993, ApJ, 410, 315
Strohmayer T. E., 1991, ApJ, 372, 573
Sturrock P. A., 1971, ApJ, 164, 529
Trümper J., Becker W., 1998, Adv. Space Res., 21, 203
Tsygan A. I., 1975, A&A, 44, 21
Unno W., Osaki Y., Ando H., Shibahashi H., 1979, Nonradial Oscillations of Stars. Univ. Tokyo Press, Tokyo
Wolfram S., 1996, The Mathematica book, third edn. Wolfram Media/ Cambridge University Press, Champaign IL

APPENDIX A: CALCULATION OF P AND δP

Substituting $\boldsymbol{B}$ from formula (26) using expansion (34) into equation (20), we have

$$\nabla\times\nabla\times\nabla\times(P_0+\delta P)\boldsymbol{e}_r=0. \tag{A1}$$

Because P does not depend on t, equation (A1) is equivalent to the following two equations:

$$\nabla\times\nabla\times\nabla\times(P_0\boldsymbol{e}_r)=0, \tag{A2}$$

$$\nabla\times\nabla\times\nabla\times(\delta P\boldsymbol{e}_r)=0. \tag{A3}$$

In spherical coordinates, equation (A3) is

$$\nabla\times\nabla\times\nabla\times(\delta P\boldsymbol{e}_r)=-\boldsymbol{e}_\theta\frac{1}{r\sin\theta}\left(\frac{1}{r^2}\partial_\phi\Delta_\Omega\delta P+\partial_{rr}\partial_\phi\delta P\right)+\boldsymbol{e}_\phi\frac{1}{r}\left(\frac{1}{r^2}\partial_\theta\Delta_\Omega\delta P+\partial_{rr}\partial_\theta\delta P\right)=0. \tag{A4}$$

Substituting the expansion of δP (35), we obtain

$$-\frac{1}{r^2}l(l+1)\delta\tilde{p}_{lm}(r,t)+\partial_{rr}\delta\tilde{p}_{lm}(r,t)=0. \tag{A5}$$

The solution of equation (A5) that vanishes at infinity is

$$\delta\tilde{p}_{lm}(r,t)=\left(\frac{r_*}{r}\right)^l\delta p_{lm}(t). \tag{A6}$$

The time-dependent coefficients $p_{lm}(t)$ have to be determined from the boundary conditions. Substituting expression (A6) into expansion (35) and taking the derivative with respect to t, we obtain expression (36).

Similarly, for the coefficients $P_{0\,lm}$ in the expansion of the function P_0 we have

$$P_{0\,lm}(r)=p_{lm}\left(\frac{r_*}{r}\right)^l. \tag{A7}$$

Substituting the expansion of the function P_0 in spherical harmonics into the boundary condition (11), multiplying this expression by Y^*_{lm} and integrating it over solid angle 4π, we have [compare this with formula (16) in Muslimov & Tsygan (1986)]

$$p_{lm}=\frac{r_*^2}{l(l+1)}\int_{4\pi}B_{0r}Y^*_{lm}\,\mathrm{d}\Omega, \tag{A8}$$

where Y^*_{lm} is the inverse spherical harmonic, $\int Y_{lm}Y^*_{l'm'}\,\mathrm{d}\Omega=\delta_{ll'}\delta_{mm'}$ and $\mathrm{d}\Omega=\sin\theta\,\mathrm{d}\theta\,\mathrm{d}\phi$ is the solid angle.

APPENDIX B: CALCULATION OF $\delta f_{lm}(t)$

Differentiating equation (41) with respect to ϕ and equation (42) with respect to θ, equating the results and multiplying by $1/\sin\theta$ we have

$$\begin{aligned}\left\{\frac{1}{\sin\theta}\partial_\theta[\sin\theta\,\partial_\theta(\partial_t P)]+\frac{1}{\sin^2\theta}\partial_{\phi\phi}(\partial_t P)\right\}\Big|_{r=r_*}=&-\left\{\frac{1}{r}\Delta_\Omega P\left[\frac{1}{\sin\theta}\partial_\theta(\sin\theta v_\theta)+\frac{1}{\sin\theta}\partial_\phi\ v_\phi\right]\right.\\&\left.+\left[\frac{1}{\sin\theta}\partial_\theta(\sin\theta\,\partial_r\partial_\theta P)+\frac{1}{\sin^2\theta}\partial_r\partial_{\phi\phi}P\right]v_r+\left[\frac{1}{r}\partial_\theta\Delta_\Omega P v_\theta+\frac{1}{r\sin\theta}\partial_\phi\Delta_\Omega P v_\phi\right]+\left[\partial_r\partial_\theta P\partial_\theta v_r+\frac{1}{\sin^2\theta}\partial_r\partial_\phi P\partial_\phi v_r\right]\right\}\Big|_{r=r_*}.\end{aligned} \tag{B1}$$

Simplifying equation (B1) by writing P as a sum of the two terms (34), we obtain an expression for the time-dependent part δP to first order in $\tilde{\xi}$:

$$\begin{aligned}\partial_t\Delta_\Omega\delta P|_{r=r_*}=&-\left[\left(v_r\partial_r\Delta_\Omega P_0+v_\theta\frac{1}{r}\partial_\theta\Delta_\Omega P_0+v_\phi\frac{1}{r\sin\theta}\partial_\phi\Delta_\Omega P_0\right)+\Delta_\Omega P_0\left(\frac{1}{r\sin\theta}\partial_\theta(\sin\theta v_\theta)+\frac{1}{r\sin\theta}\partial_\phi v_\phi\right)\right.\\&\left.+\left(\partial_r\partial_\theta P_0\partial_\theta v_r+\frac{1}{\sin^2\theta}\partial_r\partial_\phi P_0\partial_\phi v_r\right)\right]\Big|_{r=r_*}.\end{aligned} \tag{B2}$$

or in vector notation

$$\partial_t \Delta_\Omega \delta P|_{r=r_*} = -\{\mathbf{V}\cdot\nabla(\Delta_\Omega P_0) + \Delta_\Omega P_0(\nabla\cdot\mathbf{V}_\perp) + r^2(\nabla_\perp(\partial_r P_0)\cdot\nabla_\perp)v_r\}|_{r=r_*}, \tag{B3}$$

where $\mathbf{V}_\perp$ is the tangential part of the velocity, $\mathbf{V}_\perp = \boldsymbol{e}_\theta v_\theta + \boldsymbol{e}_\phi v_\phi$, and $\nabla_\perp$ is the angular part of the gradient: $\nabla_\perp = \boldsymbol{e}_\theta 1/r\ \partial_\theta + \boldsymbol{e}_\phi 1/(r\sin\theta)\partial_\phi$. Substituting the expansion of δP in spherical harmonics (36), multiplying the result by Y^*_{lm} and integrating it over the solid angle 4π, we obtain an expression for the coefficients of $\partial_t \delta p(t)$ (43) in the expansion of δP in spherical harmonics:

$$\partial_t \delta p_{lm}(t) = \frac{1}{l(l+1)}\int_{4\pi} \mathrm{d}\Omega Y^*_{lm}\{\mathbf{V}\cdot\nabla(\Delta_\Omega P_0) + \Delta_\Omega P_0(\nabla\cdot\mathbf{V}_\perp) + r^2[\nabla_\perp(\partial_r P_0)\cdot\nabla_\perp]v_r\}|_{r=r_*}.$$

Next we give explicit expressions for coefficients $\delta p_{lm}(t)$ for toroidal and spheroidal oscillation modes (see Unno et al. 1979). Spheroidal separation of variables gives the following expressions for components of the oscillation velocity in spherical coordinates:

$$v_r = \mathrm{e}^{-\mathrm{i}\omega t}U(r)Y_{lm}(\theta,\phi), \qquad v_\theta = \mathrm{e}^{-\mathrm{i}\omega t}V(r)\partial_\theta Y_{lm}(\theta,\phi), \qquad v_\phi = \mathrm{e}^{-\mathrm{i}\omega t}V(r)\frac{1}{\sin\theta}\partial_\phi Y_{lm}(\theta,\phi), \tag{B4}$$

where U and V are the radial and transverse velocity amplitude respectively. Substituting the velocity components (B4) into formula (43), we obtain the coefficients $\partial_t \delta p_{l'm'}(t)$ for spheroidal oscillations:

$$\partial_t \delta p_{l'm'}(t) = \frac{\mathrm{e}^{-\mathrm{i}\omega t}}{l'(l'+1)}\int_{4\pi}\mathrm{d}\Omega Y^*_{l'm'}\left\{U\left(Y_{lm}\partial_r\Delta_\Omega P_0 + \partial_\theta Y_{lm}\partial_\theta\partial_r P_0 + \frac{1}{\sin^2\theta}\partial_\phi Y_{lm}\partial_\phi\partial_r P_0\right)\right.$$
$$\left. + \frac{V}{r}\left[-l(l+1)Y_{lm}\Delta_\Omega P_0 + \partial_\theta Y_{lm}\partial_\theta\Delta_\Omega P_0 + \frac{1}{\sin^2\theta}\partial_\phi Y_{lm}\partial_\phi\Delta_\Omega P_0\right]\right\}\Big|_{r=r_*}. \tag{B5}$$

The oscillation velocity components for toroidal oscillations are

$$v_r = 0, \qquad v_\theta = \mathrm{e}^{-\mathrm{i}\omega t}W(r)\frac{1}{\sin\theta}\partial_\phi Y_{lm}(\theta,\phi), \qquad v_\phi = -\mathrm{e}^{-\mathrm{i}\omega t}W(r)\partial_\theta Y_{lm}(\theta,\phi), \tag{B6}$$

where W is transverse velocity amplitude. With the use of formula (B6), the coefficients in the expansion of $\partial_t \delta P$ for toroidal oscillations are

$$\partial_t \delta p_{l'm'}(t) = \frac{\mathrm{e}^{-\mathrm{i}\omega t}}{l'(l'+1)}\int_{4\pi}\mathrm{d}\Omega Y^*_{l'm'}\left[W\frac{1}{r\sin\theta}(\partial_\phi Y_{lm}\partial_\theta\Delta_\Omega P_0 - \partial_\theta Y_{lm}\partial_\phi\Delta_\Omega P_0)\right]\Big|_{r=r_*}. \tag{B7}$$

APPENDIX C: EXPRESSIONS FOR GOLDREICH–JULIAN CHARGE DENSITY FOR MODES (1,1), (2,0), (2,1) AND (3,3)

ρ^{11}_{GJ} for $0 \leqslant \theta \leqslant \pi$:

$$\rho^{11}_{\mathrm{GJ}} = \mathrm{e}^{-\mathrm{i}\omega t}\frac{3\sqrt{\frac{3}{2}}BW\cos(\theta)\sin(\theta)\sin(\phi)r_*^2}{8c\pi^{3/2}r^3}. \tag{C1}$$

ρ^{20}_{GJ} for $0 \leqslant \theta < \frac{\pi}{2}$:

$$\rho^{20}_{\mathrm{GJ}} = -\mathrm{e}^{-\mathrm{i}\omega t}\frac{3\sqrt{5}BWr_*^2[16r - 3r_* + 15\cos(4\theta)r_* - 12\cos(2\theta)(-4r + r_*)]}{256c\pi^{3/2}r^4\sqrt{1 - [\sin(\theta)^2 r_*/r]}}. \tag{C2}$$

ρ^{20}_{GJ} for $\frac{\pi}{2} < \theta \leqslant \pi$:

$$\rho^{20}_{\mathrm{GJ}} = \mathrm{e}^{-\mathrm{i}\omega t}\frac{3\sqrt{5}BWr_*^2[16r - 3r_* + 15\cos(4\theta)r_* - 12\cos(2\theta)(-4r + r_*)]}{256c\pi^{3/2}r^4\sqrt{1 - [\sin(\theta)^2 r_*/r]}}. \tag{C3}$$

ρ^{21}_{GJ} for $0 \leqslant \theta \leqslant \pi$:

$$\rho^{21}_{\mathrm{GJ}} = \mathrm{e}^{-\mathrm{i}\omega t}\frac{\sqrt{\frac{5}{6}}BW\sin(\theta)\sin(\phi)r_*^{3/2}[21r + 19r_* + 45\cos(2\theta)r_*]}{32c\pi^{3/2}r^{7/2}}. \tag{C4}$$

ρ^{33}_{GJ} for $0 \leqslant \theta < \frac{\pi}{2}$:

$$\rho^{33}_{\mathrm{GJ}} = \mathrm{e}^{-\mathrm{i}\omega t}\frac{3\sqrt{35}BW\sin(\theta)^3\sin(3\phi)r_*^{5/2}}{256c\pi^{3/2}r^{11/2}\sqrt{1 - [\sin(\theta)^2 r_*/r]}}[15r^2 + 2rr_* + 6\cos(4\theta)r_*^2 - 6\cos(2\theta)r_*(-5r + r_*)$$
$$- 6\sqrt{2}\cos(3\theta)r_*^{3/2}\sqrt{2r - r_* + \cos(2\theta)r_*}]. \tag{C5}$$

$\rho^{33}_{\rm GJ}$ for $\frac{\pi}{2} < \theta \leqslant \pi$:

$$\rho^{33}_{\rm GJ} = -\mathrm{e}^{-\mathrm{i}\omega t}\frac{3\sqrt{35}BW\sin(\theta)^3\sin(3\phi)r_*^{5/2}}{256c\pi^{3/2}r^{11/2}\sqrt{1-[\sin(\theta)^2 r_*/r]}}[15r^2+2rr_*+6\cos(4\theta)r_*^2-6\cos(2\theta)r_*(-5r+r_*)$$
$$+6\sqrt{2}\cos(3\theta)r_*^{3/2}\sqrt{2r-r_*+\cos(2\theta)r_*}]. \qquad \text{(C6)}$$

This paper has been typeset from a TEX/LATEX file prepared by the author.